Superdeformed band at very high spin in ^{140}Nd

A. Neußer, H. Hübel, A. Al-Khatib, P. Bringel, A. Bürger, N. Nenoff, G. Schönwaßer, and A. K. Singh*
Helmholtz-Institut für Strahlen- und Kernphysik, Universität Bonn, Nußallee 14-16, D-53115 Bonn, Germany

C. M. Petrache and G. Lo Bianco
Dipartimento di Fisica, Università di Camerino and INFN, Sez. Perugia, I-62032, Camerino, Italy

I. Ragnarsson
Department of Mathematical Physics, Lund Institute of Technology, S-22362 Lund, Sweden

G. B. Hagemann, B. Herskind, D. R. Jensen, and G. Sletten
Niels Bohr Institute, Blegdamsvej 17, DK-2100 Copenhagen, Denmark

P. Fallon and A. Görgen†
Nuclear Science Division, Lawrence Berkeley National Laboratory, Berkeley, California 94720, USA

P. Bednarczyk‡ and D. Curien
Institut de Recherches Subatomiques, 23 Rue du Loess, F-67037 Strasbourg, France

G. Gangopadhyay
Department of Physics, University College of Science, 92 A.P.C. Road, Kolkata 700009, India

A. Korichi and A. Lopez-Martens
Centre de Spectrometrie Nucleaire et de Spectrometrie de Masse, F-91405 Orsay Campus, France

B. V. T. Rao and T. S. Reddy
Department of Nuclear Physics, Andhra University, Visakhapatnam 530003, India

Nirmal Singh
Department of Physics, Panjab University, Chandigarh 160014, India
(Received 11 August 2004; published 16 December 2004)

A new high-spin superdeformed band has been discovered in $^{140}_{60}Nd_{80}$. It was populated in the ^{96}Zr(^{48}Ca,$4n$) reaction and investigated using the EUROBALL γ-ray spectrometer array. The band is observed in the approximate spin range of $I=36$ to 66. It is associated with shell gaps around $Z=60$ and at $N=80$ at large deformation. These gaps produce a pronounced minimum in the calculated total Routhian surfaces at a quadrupole deformation of $\epsilon_2=0.45$. The new band which lies between the high-deformation bands in the $A\approx130$ region and the superdeformed bands in $A\approx150$ nuclei provides insight into the development of the deformation between these two regions. Two possible configurations are suggested involving four neutrons of $i_{13/2}$ origin ($\nu 6^4$) and either six protons of $h_{11/2}/h_{9/2}$ origin ($\pi 5^6$) or five protons of $h_{11/2}/h_{9/2}$ and one of $i_{13/2}$ origin ($\pi 5^5 6^1$).

DOI: 10.1103/PhysRevC.70.064315 PACS number(s): 21.10.Re, 21.60.Ev, 23.20.Lv, 27.60.+j

I. INTRODUCTION

The coexistence of excited states with different shapes is a well known phenomenon in atomic nuclei. In the mass region of $A\approx130$–150, shape coexistence has been investigated extensively, both theoretically and experimentally. Potential-energy surface calculations predict a variety of minima and, indeed, spherical or low-deformation minima are found to coexist with oblate, triaxial, highly deformed or superdeformed minima. At high spins the second or third wells in the total Routhian surfaces with very large deformation usually become more pronounced than at low spin. Figure 1 shows an example of the calculations for ^{140}Nd which is the subject of the present investigation. The total Routhian surfaces have been calculated using the Ultimate Cranker (UC) code [1,2]. A near-spherical minimum, which is still yrast at spin 36, is observed to coexist with local minima with large triaxiality and with a superdeformed well at $\epsilon_2=0.45$. At very high spins, the low-deformation minimum

*Present address: Department of Physics, IIT Kharagpur, Kharagpur-721302, India.
†Present address: DAPNIA/SPhN, CEA Saclay, F-91191 Gif-sur-Yvette, France.
‡Present address: Gesellschaft für Schwerionenforschung, Planckstr. 1, D-64291 Darmstadt, Germany.

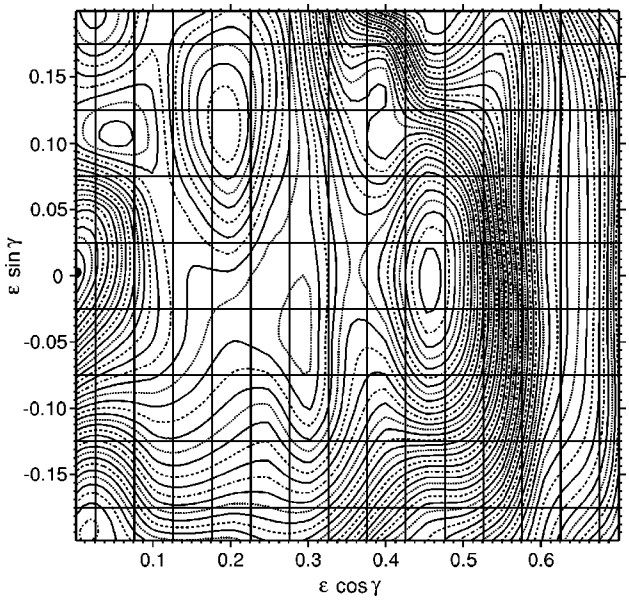

FIG. 1. Total Routhian surface of ^{140}Nd, calculated with the Ultimate Cranker code for angular momentum $I=36$ and $(\pi,\alpha)=(+,0)$. The energy difference between the contour lines is 0.2 MeV. The superdeformed minimum with $\epsilon_2=0.45$ becomes more pronounced at higher spins.

moves to the oblate noncollective axis while the prolate superdeformed minimum becomes more pronounced.

A large number of rotational bands that can be associated with the different minima have been found throughout the entire mass region [3–5]. The predicted shape coexistence has been confirmed by lifetime measurements from which quadrupole moments have been deduced. The bands which show small moments of inertia, and small quadrupole moments, have been associated with low-deformation and/or triaxial potential-energy minima; see e.g. [6–8]. At the lower end of the mass region, near $A=130$, the second wells have moderate deformations, but at the upper end, near $A=150$, these minima are superdeformed ($\epsilon_2\approx 0.6$) corresponding to nuclear axis ratios of about 2:1; see e.g. [9–13]. A full understanding of the variation of the deformation of the second well with increasing Z and N, going from the $A=130$ to the $A=150$ region, is of great interest for nuclear structure physics. While a lot of experimental information exists at both ends of this mass range, data are lacking in the center of the region. The present work on ^{140}Nd is an important contribution in this respect.

This nucleus lies in the middle of this mass region where it is interesting to locate the shell gaps that are responsible for the second well at large deformation. In the lighter nuclei the shell gaps around $Z=60$ (Ce, Nd) and $N=72,74$ produce the highly-deformed minima, while in the heavier nuclei the gaps at $Z=64$ (Gd), 66 (Dy) and $N=86,88$ form the superdeformed wells. It is, furthermore, important information on the location of the deformation-driving intruder orbitals that are occupied by excited nucleons in the second well.

In this paper, we report on the first observation of a high-spin superdeformed band in ^{140}Nd. Previously, only low-deformation states up to spin 17 were known in this nucleus [14].

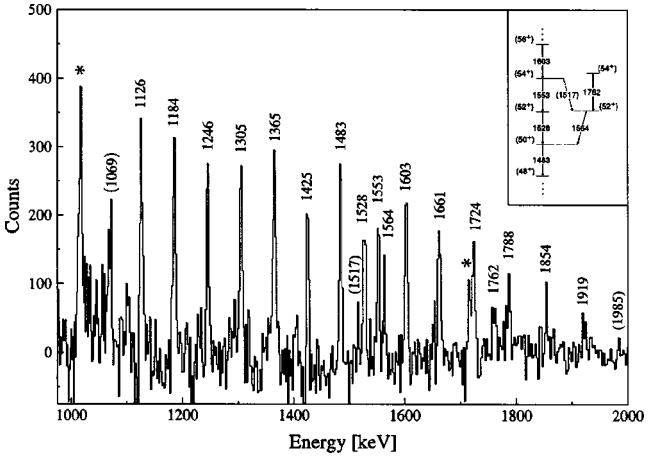

FIG. 2. Gamma-ray coincidence spectrum of the new superdeformed rotational band in ^{140}Nd. The spectrum was obtained by summing all spectra obtained from combinations of double gates on transitions from the list of energies 1126, 1184, 1246, 1305, 1365, 1425, 1483, 1603, and 1661 keV. The transitions marked with asterisks are low-lying transitions in ^{140}Nd.

II. EXPERIMENTAL DETAILS

High-spin states in ^{140}Nd have been populated in the reaction ^{96}Zr(^{48}Ca, $4n$) at 195 MeV at the Vivitron tandem accelerator at IReS, Strasbourg. A self-supporting ^{96}Zr foil of 735 μg/cm^2 thickness was used as a target. Gamma-ray coincidences were measured with the EUROBALL spectrometer array [15], consisting of 30 single, tapered Ge detectors, 15 Cluster and 26 Clover composite Ge detectors. Each of them was surrounded by a BGO Compton-suppression shield. Out of a maximum total of 239 Ge crystals, 230 could be used in our analysis. Multiplicity information was obtained from the inner ball of 210 BGO detectors. Events were written to tape with the requirement that at least 11 BGO detectors of the inner ball and four Ge crystals before Compton suppression were in prompt coincidence. Presorting of the data which included Compton suppression and add-back for the composite detectors resulted in a total of 1.5×10^9 events with a γ-ray coincidence fold of $f\geqslant 3$.

The γ-ray coincidences were sorted into three- and four-dimensional coincidence arrays (cube and hypercube, respectively), and the analysis was carried out using the RADWARE software package [16]. The analysis revealed a previously unknown [14] rotational band with a large moment of inertia in ^{140}Nd. The γ-ray coincidence spectrum of the new band is displayed in Fig. 2. The band is very regular with an average energy spacing between the transitions of 61 keV, except for one irregularity around a transition energy of 1550 keV. The assignment of the band to ^{140}Nd is unambiguous since transitions between levels up to spin 26 in this nucleus are observed in coincidence with the band. However, no direct linking transitions between the band and the lower-lying states have been found, probably due to the fragmentation of the decay and the low intensity of the decay branches. Note that the intensity of the band is estimated to be only about 1% of the $4n$ reaction channel leading to ^{140}Nd.

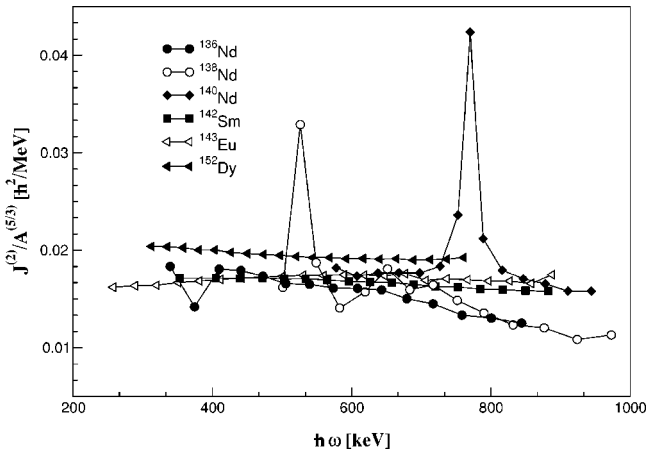

FIG. 3. Dynamic moment of inertia, $J^{(2)}$, for the new band in ^{140}Nd compared to those of similar bands in neighboring isotopes and isotones. For a better comparison the values are scaled by $A^{5/3}$. References are given in the text.

To determine the multipolarity of the in-band transitions, two gated matrices were sorted with all detectors on one axis and detectors at 90 degree and at forward/backward angles, respectively, on the other axis. Gates on the transitions of the band were set on the axis with all detectors and the intensity ratio $W(f,b)/W(90)$ was determined for several in-band transitions from the resulting spectra. Although the errors are large due to the low statistics, the results are consistent with stretched quadrupole, probably $E2$, transitions.

The dynamic moment of inertia of the new band is compared to those of known bands in Nd isotopes [17–19], in the isotones $^{142}_{62}Sm_{80}$ [20] and $^{143}_{63}Eu_{80}$ [21] and in $^{152}_{66}Dy_{86}$ [22] in Fig. 3. For a mass-independent comparison the moments of inertia are scaled by $A^{5/3}$. The moment of inertia of the ^{140}Nd band lies rather close to that of the isotone ^{143}Eu. At a rotational frequency of $\hbar\omega=0.77$ MeV, ^{140}Nd shows a band crossing with a gain in alignment of about $2\hbar$ which the lighter Nd isotopes and the heavier isotones do not show. In the crossing region two levels of the same spin and parity are close in energy, shown as $I^{\pi}=52^{+}$ states in the inset to Fig. 2. The mixing of these levels could explain the occurrence of the tentative transition of 1517 keV out of the band and the one of 1564 keV into the band. The state with which the band mixes probably belongs to a low-deformation band because the energy-level spacing of 1762 keV is larger than that of the superdeformed band at the same spin and is probably even larger if the level repulsion was removed. Unfortunately, a mixing calculation could not be performed because the intensity of the tentative 1517 keV transition could not be determined with sufficient accuracy. Due to the low intensity no further levels of the low deformation band could be observed.

Since the new superdeformed band is not linked to lower levels, the excitation energy, spins and parity cannot be determined directly. To estimate the spins, we have used the spin-fitting methods described in Refs. [23–26] which result in $I_0=(36\pm2)$ for the lowest level of the band, that could be firmly established. This is consistent with the spin-transition-energy relation of the other strongly deformed bands in the neighboring nuclei, ^{136,138}Nd [18,19] and ^{143}Eu [21]. However, it cannot be excluded that an alignment at lower spin could change this value. If the spin assignment is correct, the new band is observed from spin 36 to 66. The 1069 and 1985 keV lines, shown as tentative band members in Fig. 2, may possibly be the $36\rightarrow34$ and $68\rightarrow66$ transitions, respectively. Thus, it differs from the bands in the lighter Nd isotopes in two ways: the decay-out occurs at higher spins and, despite its low intensity, it is observed to very high spins. The bands in the lighter isotopes extend to much lower frequencies, corresponding to spins 25/2, 17 and 26-28 for ^{135}Nd [27], ^{136}Nd [18] and ^{138}Nd [19], respectively. With the present spin assignment, the excitation energy of the lowest observed level of the band is estimated to be around 19 MeV from a plot of the energies of all known levels in ^{140}Nd as a function of spin.

As in our experiment a thin target of 735 μg/cm^2 thickness was used we cannot do a proper Doppler-shift lifetime analysis to derive the quadrupole moment from the transition probabilities. However, the transition energies of the new band are high, between 1126 and 1919 keV, and due to the E^5 dependence of the $E2$-transition probabilities the lifetimes are expected to be so short that a considerable fraction of the γ rays are emitted from nuclei which are still recoiling through the target. Therefore, along the band these transitions show different Doppler shifts corresponding to different velocities of the recoiling nuclei as they are slowed down in the target. This effect can be used to obtain an estimate of the lifetimes [28]. For this purpose, coincidence spectra of the band were sorted with 13 different recoil velocities between the full velocity calculated from the reaction kinematics for a beam energy of 191 MeV at the middle of the target, $v_{max}/c=0.0308$, and the velocity of the recoils after they have left the target, $v_{min}/c=0.0284$. The latter was determined from transitions between low-lying states with longer lifetimes decaying in vacuum. The full width at half maximum (FWHM) of the peaks in these 13 coincidence spectra was then determined for 10 transitions in the band. The smallest FWHM corresponds to the correct average velocity $\overline{v}$ at the time of emission of the γ rays. The fractional shifts, $\overline{v}/v_{max}$, are plotted as a function of transition energy in Fig. 4. A fit of calculated shifts to these data results in a transition quadrupole moment of $Q_t=9.0^{+3.7}_{-2.0}$ b. For a comparison the curves for the upper and lower limits given by the uncertainty of the quadrupole moment are included. The stopping powers of Ziegler *et al.* [29] were used for these calculations. The uncertainty introduced by insufficient knowledge of the stopping powers is not included in the experimental error. The side feeding was modeled by a rotational cascade with a constant quadrupole moment, Q_{sf}, which was assumed to be equal to that of the in-band transitions, $Q_{sf}=Q_t$. The intensities of the side feeding transitions were determined from the intensity profile of the band.

III. DISCUSSION

Both the moment of inertia and the quadrupole moment of the new band are larger than those for the lighter-mass Nd isotopes and more similar to the heavier isotones. In the

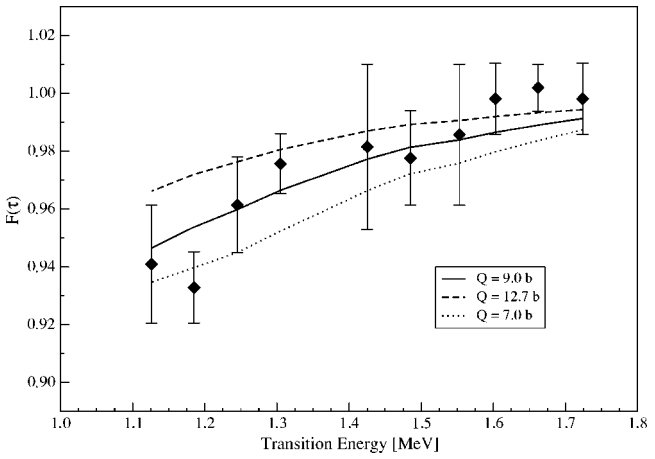

FIG. 4. Fractional Doppler shifts determined for 10 transitions of the superdeformed band in ^{140}Nd (see text). Calculated shifts for different quadrupole moments are shown for comparison.

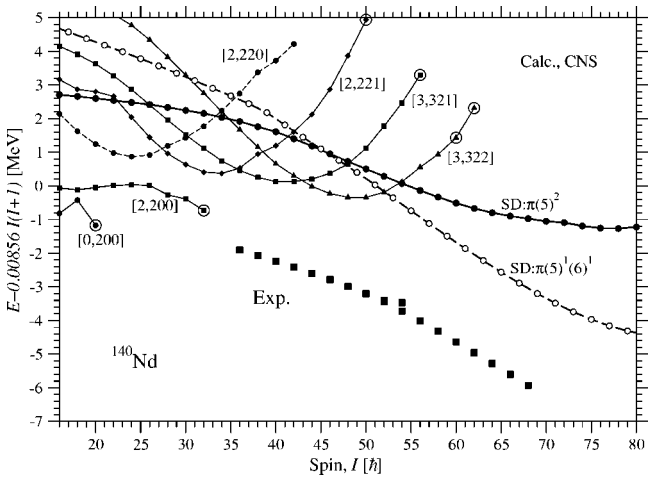

FIG. 5. Energies of the new superdeformed band in ^{140}Nd compared to calculations for different configurations. For the calculated bands, full and open symbols are used for even and odd spins, respectively, and full and dashed lines indicate positive and negative parity, respectively. In addition to the two superdeformed bands, typical "close-to-spherical" and triaxial lower-spin bands are shown. The experimental band is plotted assuming $I=36$ for the lowest observed level. The absolute energy scale is arbitrary. Thus, only the slope and curvature are relevant when comparing experiment with theory.

chain of the lighter Nd isotopes, the quadrupole moments are decreasing with increasing mass number [30]. This trend has been explained by an increase in γ deformation of the highly deformed minima at $\epsilon_2 \approx 0.30$ from $\gamma=0°$ towards 30° [31]. Most recently, a band was found in ^{138}Nd [19] which was associated with the minimum at $\epsilon_2=0.28$ and $\gamma=30°$. For the new band in ^{140}Nd with the larger moment of inertia and the larger quadrupole moment we suggest that it belongs to the axially symmetric superdeformed minimum at $\epsilon_2=0.45$ observed in the total Routhian calculations, see the example displayed in Fig. 1. This minimum is well pronounced at high spin, but lies higher in energy and becomes less pronounced at lower spins. It should be noted that the lowest spin to which we can actually observe the band in our experiment is $I_0=(36\pm2)$.

For a configuration assignment to the new band we have performed configuration-dependent cranked Nilsson-Strutinsky calculations [32,33], using the same single-particle parameters as in Ref. [31]. In Fig. 5 the excitation energy of the experimental band relative to a rigid-rotor reference is compared to the result of these calculations. As the calculations do not include pairing, they cannot be used to calculate the ground state and, therefore, do not predict the excitation energy of the high-spin bands and the absolute energy scale between calculations and experiment is arbitrary.

From the calculations, two low-lying superdeformed configurations and several normal-deformed triaxial configurations are shown. The labeling of the normal-deformed bands in Fig. 5 is as explained in Ref. [33]. The first number in the square brackets gives the number of $h_{11/2}$ protons, while the three numbers after the comma define the neutron configuration: first the number of $h_{11/2}$ neutron holes followed by the number of $(h_{9/2}, f_{7/2})$ and $i_{13/2}$ neutrons, respectively. Two superdeformed bands appear at low energy in the calculations. They are labeled by the N-shells of the two protons above the $Z=58$ gap at $\epsilon_2 \approx 0.4$ seen in Fig. 6: $\pi(5)^2$ for a positive-parity even-spin band and $\pi(5)^1(6)^1$ for a negative-parity odd-spin band. Since the parity of the SD band is not determined experimentally and the spin values are uncertain within ± 2 ħ, both alternatives are possible candidates for the configuration. The slope of the $(\pi,\alpha)=(+,0)$ $\pi(5)^2$ configuration compares well to that of the observed band in the lower spin region. In total, this configuration contains four neutrons in the strongly deformation-driving $i_{13/2}$ orbitals (6^4) and six protons in $h_{11/2}$ orbitals (5^6). The change in slope in the calculation around spin 40 is caused by the excitation of an $h_{11/2}$ proton into the lowest $h_{9/2}$ orbital. In

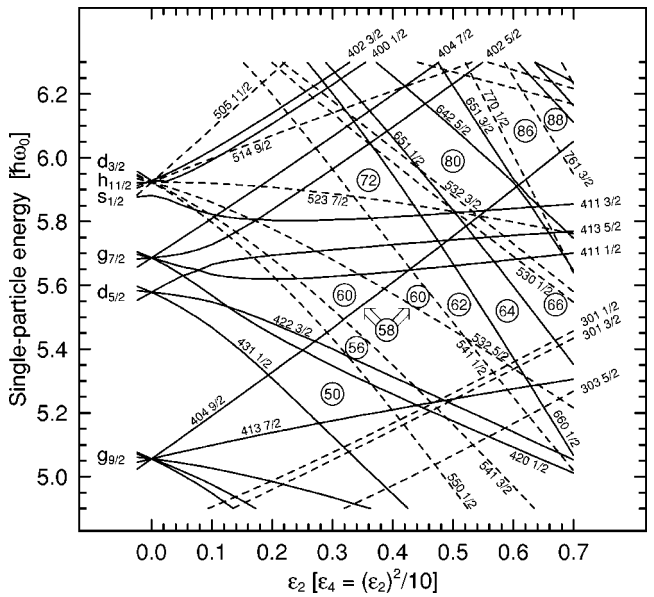

FIG. 6. Calculated single-particle energies as a function of quadrupole deformation ϵ_2, with a small hexadecapole deformation ϵ_4 which is proportional to $(\epsilon_2)^2$.

Nilsson quantum numbers, this may be expressed as an excitation from the $[532]5/2$ to the $[541]1/2$ orbital with a small gain in alignment. Experimentally, this crossing is observed at $\hbar\omega = 0.77$ MeV, see Fig. 3, with a gain in alignment of 2 $\hbar$. It lies at higher spin than in the calculation, but the crossing frequency is strongly dependent on the relative position of the $h_{11/2}$ and $h_{9/2}$ proton subshells which is not well established. Indeed, the present crossing is a good measure of this distance and, thus, could be used to improve the single-particle parameters in the calculation. This crossing is neither observed in the heavier isotones nor in the lighter isotopes. In the heavier isotones with $Z > 60$ the $[541]1/2$ orbital is already occupied and, therefore, the excitation is blocked. In the lighter isotones this excitation takes more energy, because at lower deformation and with $\gamma \approx 30°$ the strongly down-sloping $[541]1/2$ orbital lies rather high above the Fermi level.

At high spins, the $(\pi, \alpha) = (-, 1)$ superdeformed configuration $\pi(5)^1(6)^1$ appears even lower in energy than the $(+, 0)$ band in the calculation. In total, it contains five protons in the $h_{11/2}$ orbital (5^5) and one in the $i_{13/2}$ orbital (6^1) in addition to the four neutrons in $i_{13/2}$ orbitals (6^4). The observed alignment may in this case also be explained by the excitation of an $h_{11/2}$ proton ($[532]5/2$) into an $h_{9/2}$ ($[541]1/2$) orbital. The calculated slope agrees well with the observed slope in the upper part of the band. This is the region where the calculation should be more reliable since pairing is neglected. The negative parity and odd spins of this configuration might seem strange, but such a configuration has also been assigned to the yrast SD band in ^{142}Sm [34]. The calculated average quadrupole moments for both configurations, $Q = 10.9$ and 11.1 b for the positive-parity/even-spin and the negative-parity/odd-spin band, respectively, are slightly larger than the value estimated from the Doppler shifts, but are both in agreement with the experimental value within the limits of error. The calculated quadrupole moment is similar to those observed and calculated in SD bands in the isotones ^{142}Sm [20] and ^{143}Eu [35].

The development of the deformation in the second well in the total Routhian surfaces going from $A = 130$ to $A = 150$ can nicely be explained by the location of the shell gaps in the single-particle Routhians and by the occupation of the different deformation-driving orbitals. The single-particle energy diagram shown in Fig. 6 is calculated for neutrons but can also be used for protons to illustrate the development of the orbitals as a function of deformation and particle number. The energy gaps pointed out in the following are also seen in the calculated single-particle Routhians. For the $_{58}$Ce isotopes the large gap at $Z = 58$ and the gaps at $N = 72, 74$ determine the large deformation. When two protons are added, they can either be placed in the up-sloping $[404]9/2$ orbital or in the down-sloping $N = 5$ or $N = 6$ orbitals leading to the two $Z = 60$ gaps indicated in Fig. 6. When combined with the neutron orbitals, the small deformation gap at $Z = 60$ appears to be preferred for the lighter $_{60}$Nd isotopes up to $N = 78$, resulting in a moderate deformation and with a tendency towards triaxiality. In $^{140}_{60}Nd_{80}$, however, a large gap at $N = 80$ opens up at a large deformation. When combined with the $Z = 60$ gap, it leads to the superdeformed band discussed here. Going up in proton and neutron numbers into the $A = 150$ region, the $Z = 64, 66$ and $N = 86, 88$ shell gaps are close to the Fermi level at very large deformation. Here, quadrupole deformation parameters of about 0.6 and axis ratios of $c:a \approx 2:1$ are observed. The nuclei $^{149}_{64}Gd_{85}$ and $^{152}_{66}Dy_{86}$ are well-known examples [13]. In Fig. 6, one notes the crossing around $Z = 60$ between the $[541]1/2$ and $[532]5/2$ orbitals. It is the interaction between these orbitals at a finite rotational frequency which explains the crossing in the band observed in ^{140}Nd. One can then note the analogous crossing one shell up between the $[642]5/2$ and $[651]3/2$ neutron orbitals which in a similar way explains the alignments observed in $^{146\text{-}148}$Gd [36]. Thus, the result presented in the present work is an important link that was missing in the understanding of the properties and, in particular, the different deformations of superdeformed bands in the $A = 130$–150 mass region.

IV. SUMMARY

In summary, we have observed a new rotational band with a large moment of inertia and a large quadrupole moment in ^{140}Nd. It is associated with the superdeformed minimum found in potential-energy calculations. Two possible configurations are suggested involving four neutrons of $i_{13/2}$ origin $(\nu 6^4)$ and either six protons of $h_{11/2}/h_{9/2}$ origin $(\pi 5^6)$ or five protons of $h_{11/2}/h_{9/2}$ and one of $i_{13/2}$ origin $(\pi 5^5 6^1)$. It shows a small alignment gain around spin 52 which is probably caused by an excitation of a $h_{11/2}$ proton into the $h_{9/2}$ orbital. The properties of the band confirm the expectation that the deformation of the bands increases from the $A = 130$ to the $A = 150$ mass region because the shell gaps responsible for the potential-energy minima appear at increasing deformations.

ACKNOWLEDGMENTS

The authors are grateful to the technical staff at IReS involved in running the Vivitron accelerator and the EUROBALL array. The work was supported by BMBF, Germany, under Contract No. 06 BN 907, by the EU under Contract No. HPRI-CT-1999-00078, by the Italian National Institute of Nuclear Physics (INFN), by the Danish Science Foundation, by the Swedish Science Research Council and by DOE under Contract No. DE-AC03-76SF00098.

[1] R. Bengtsson: http://www.matfys.lth.se/~ragnar/ultimate.html
[2] T. Bengtsson, Nucl. Phys. **A496**, 56 (1989); **A512**, 124 (1990).
[3] B. Singh, R. Zywina, and R. B. Firestone, Nucl. Data Sheets **97**, 241 (2002).
[4] X. L. Han and C. L. Wu, At. Data Nucl. Data Tables **63**, 117 (1996).
[5] R. B. Firestone, in *Table of Isotopes*, edited by V. S. Shirley *et al.* (Wiley, New York, 1999).
[6] D. T. Joss *et al.*, Phys. Rev. C **58**, 3219 (1998).
[7] N. J. O'Brien, A. Galindo-Uribarri, V. P. Janzen, D. T. Joss, P. J. Nolan, C. M. Parry, E. S. Paul, D. C. Radford, R. Wadsworth, and D. Ward, Phys. Rev. C **59**, 1334 (1999).
[8] C. M. Petrache *et al.*, Phys. Rev. C **61**, 011305 (1999).
[9] C. M. Petrache *et al.*, Phys. Rev. C **57**, R10 (1998).
[10] C. M. Petrache *et al.*, Phys. Lett. B **219**, 145 (1996).
[11] F. G. Kondev *et al.*, Phys. Rev. C **59**, 3076 (1999).
[12] M. A. Bentley *et al.*, Phys. Rev. Lett. **59**, 2141 (1987).
[13] H. Savajols *et al.*, Phys. Rev. Lett. **76**, 4480 (1996).
[14] E. Gülmez, H. Li, and J. A. Cizewski, Phys. Rev. C **36**, 2371 (1987).
[15] J. Simpson, Z. Phys. A **358**, 139 (1997).
[16] D. C. Radford, Nucl. Instrum. Methods Phys. Res. A **361**, 297 (1995).
[17] C. M. Petrache, Z. Phys. A **358**, 225 (1997).
[18] S. Perriès *et al.*, Phys. Rev. C **60**, 064313 (1999).
[19] S. Lunardi *et al.*, Phys. Rev. C **69**, 054302 (2004).
[20] G. Hackman, R. V. F. Janssens, E.. F. Moore, D. Nisius, I. Ahmad, M. P. Carpenter, S. M. Fischer, T. L. Khoo, T. Lauritsen, and P. Reiter, Phys. Lett. B **416**, 268 (1998).
[21] A. Ataç *et al.*, Phys. Rev. Lett. **70**, 1069 (1993).
[22] T. Lauritsen *et al.*, Phys. Rev. Lett. **89**, 282501 (2002).
[23] J. E. Draper *et al.*, Phys. Rev. C **42**, R1791 (1990).
[24] J. A. Becker *et al.*, Phys. Rev. C **46**, 889 (1992).
[25] C. S. Wu, J. Y. Zeng, Z. Xing, X. Q. Chen, and J. Meng, Phys. Rev. C **45**, 261 (1992).
[26] C. S. Wu, L. Cheng, C. Z. Lin, and J. Y. Zeng, Phys. Rev. C **45**, 2507 (1992).
[27] M. A. Deleplanque *et al.*, Phys. Rev. C **52**, R2302 (1995).
[28] B. Cederwall *et al.*, Nucl. Instrum. Methods Phys. Res. A **354**, 591 (1995).
[29] J. F. Ziegler, J. P. Biersack, and U. Littmark, *The Stopping and Ranges of Ions in Matter* (Pergamon, London, 1985).
[30] F. G. Kondev *et al.*, Phys. Rev. C **60**, 011303 (1999).
[31] A. V. Afanasjev and I. Ragnarsson, Nucl. Phys. **A608**, 176 (1996).
[32] T. Bengtsson and I. Ragnarsson, Nucl. Phys. **A436**, 14 (1985).
[33] A. V. Afanasjev, D. B. Fossan, G. J. Lane, and I. Ragnarsson, Phys. Rep. **322**, 1 (1999).
[34] G. Hackman, S. M. Mullins, J. A. Kuehner, D. Prévost, J. C. Waddington, A. Galindo-Uribarri, V. P. Janzen, D. C. Radford, N. Schmeing, and D. Ward, Phys. Rev. C **47**, R433 (1993).
[35] S. A. Forbes, A. Ataç, G. B. Hagemann, B. Herskind, S. M. Mullins, P. J. Nolan, J. Nyberg, M. J. Piiparinen, G. Sletten, and R. Wadsworth, Nucl. Phys. **A584**, 149 (1995).
[36] I. Ragnarsson, Nucl. Phys. **A557**, 167c (1993).